

Robust dynamical decoupling with concatenated continuous driving

J.-M. Cai,¹ F. Jelezko,² M. B. Plenio,¹ and A. Retzker¹

¹*Institut für Theoretische Physik, Albert-Einstein Allee 11, Universität Ulm, 89069 Ulm, Germany*

²*Institut für Quantenoptik, Albert-Einstein Allee 11, Universität Ulm, 89069 Ulm, Germany*

(Dated: September 4, 2022)

The loss of coherence is one of the main obstacles for the implementation of quantum information processing. Here we introduce the concept of concatenated continuous dynamical decoupling, which can overcome not only external noise but also fluctuations in driving fields that implement the decoupling sequences and thus holds the potential for achieving relaxation limited coherence times. The proposed scheme can be applied to a wide variety of physical systems including, trapped atoms and ions, quantum dots and nitrogen-vacancy (NV) centers in diamond, and may be combined with other quantum technologies challenges such as quantum sensing or quantum information processing.

Introduction.— Coherent control of quantum systems has opened a promising route towards novel quantum devices for quantum technologies, such as quantum information processing, quantum metrology and quantum sensing [1–4]. The performance of such quantum devices critically depends on coherence times of their constituent quantum systems which, in turn, is limited due to uncontrolled interactions with their surrounding environment [5]. This results in the challenging but fundamentally important task in current quantum experiments, namely how to protect individual quantum states from decoherence by their environment while retaining the ability to control the quantum dynamics of the system, in particular for solid state with characteristic complex environments. The method of dynamical decoupling has been introduced to overcome decoherence without the need for redundancy that is required in quantum error correction schemes. In standard pulsed dynamical decoupling schemes [6, 7], one uses a series of sharp pulses to reduce the decoherence coming from the undesired interaction with the environment. Dynamical decoupling has become a standard tool in liquid state NMR allowing to resolve complex spectra of proteins. Significant progress has been made with the theoretical proposals of various dynamical decoupling protocols [8–13], and their experimental demonstrations [14–20]. Despite these successes, pulsed schemes suffer physical limitations due to, for example, the limited achievable repetition rate of pulses and relative complexity of combining these schemes with other quantum information tasks.

These challenges can be addressed by decoupling schemes that require only continuous oscillatory driving fields. These approaches inherit the advantages of standard dynamical decoupling, namely requiring no encoding overhead, no quantum measurements, and no feedback controls. Moreover, they are not subject to the physical limit for pulsed dynamical decoupling and are more naturally combined with other quantum information tasks. Recent work has demonstrated that continuous dynamical decoupling can protect qubits from magnetic field fluctuations and allow to perform high fidelity quantum gates [11–13, 20]. In principle, one can apply

continuous driving to reduce the noise suffered by a qubit considerably. The coherence time, however remains limited by both random and systematic fluctuation in the driving field itself.

Here we address this remaining challenge by introducing two schemes of concatenated continuous decoupling (CCD), which can significantly extend coherence times by protecting against the fluctuations in the driving fields themselves. Our basic idea includes amplitude locking and recursive driving in order to reduce the dephasing effect to a higher order of fluctuation. We demonstrate that these schemes can be implemented in two- and three level quantum systems and employ numerical simulations to verify that our CCD schemes can increase coherence times by several orders of magnitude as compared to standard schemes based on a single drive. Our proposed CCD schemes can find applications in a wide variety of quantum systems, among them, trapped atoms or ions and quantum dots. Here we concentrate on the particularly appealing application of our schemes to NV centers in diamond. It is known that the electron spin state of NV center can be optically initialized, read out, and coherently controlled at room temperature [21]. Basic quantum information processing protocols, as well as ultrasensitive magnetometry have been demonstrated at room temperature [22–24]. The main decoherence of NV center stems from the interaction of the electron spin with electron spin bath for nitrogen-rich crystals and nuclear spin bath for isotopically purified diamond [17, 25, 26], which induces an effective fluctuating magnetic field on the electron spin, while the spin relaxation time is very long even at room temperature. Significant progress was achieved in material engineering [27]. However not all source of magnetic noise can be eliminated, in particular for implanted NV defects [24]. Using concatenated continuous dynamical decoupling, the coherence time can in principle approach the spin relaxation time. With such an ultralong coherence time, our results will be beneficial for the construction of quantum memory [28], highly sensitive nano-scale magnetometer [1–3] and fault-tolerant quantum operation.

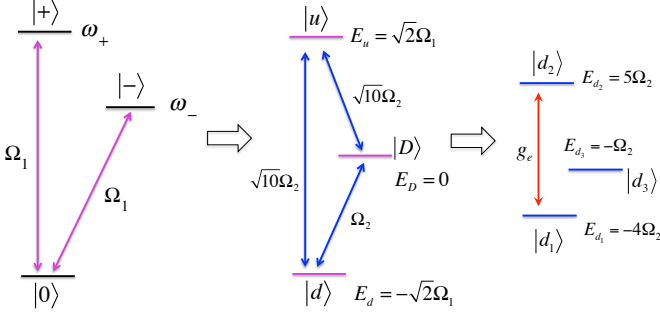


FIG. 1. Amplitude-lock continuous dynamical decoupling: The first-order driving (left, purple) creates the dress states $|u\rangle$, $|D\rangle$, $|d\rangle$ (middle) which are decoupled from dephasing noise but suffer from the fluctuation in the driving field itself. The second-order driving (middle, blue) acting on the first-order dressed states leads to concatenated dressed states (right) that are immune to both dephasing noise and the intensity fluctuations of driving fields. The numbers beside the transition arrows denote the Rabi frequencies.

Amplitude-lock continuous dynamical decoupling — We start by considering a three-level quantum system with the eigenstates $|0\rangle, |\pm\rangle$, the latter with energies ω_+ and ω_- , see Fig.1(a). Environmental noise causes fluctuations to the energies ω_{\pm} and thus the loss of coherence. To counter such effects, we can apply driving fields on resonance with the energy gap between $|0\rangle$ and $|\pm\rangle$. A qubit can then be encoded with the corresponding dressed states $|u\rangle = \frac{1}{2}(|+\rangle + |-\rangle) + \sqrt{2}|0\rangle$, $|D\rangle = \frac{1}{\sqrt{2}}(|+\rangle - |-\rangle)$, $|d\rangle = \frac{1}{2}(|+\rangle + |-\rangle - \sqrt{2}|0\rangle)$. In this basis, the effect of dephasing now induces transitions among these dressed states, which is suppressed by an energy penalty and are thus strongly suppressed as long as the noise power spectrum at the resonance frequency is negligible [20]. The above analysis is based on the assumption that the amplitude of the driving fields is constant. In realistic experiments however, the intensity of the driving fields will fluctuate owing to limited stability of microwave sources and amplifiers (the frequency instead can be relatively much more stable), and thus cause fluctuations of the dressed states. Achievable coherence times are thus ultimately limited by the stability of the driving fields [29]. To overcome such a systematic problem, we introduce a second-order continuous driving on resonance with the transitions between the first-order dressed states. The intensity of the second-order driving fields is subject to fluctuations too. Nevertheless, if these fields are derived from the same power source (e.g. via sidebands) they will be strongly correlated, namely $\delta\Omega_i(t) = \Omega_i\delta(t)$ where $\delta(t)$ denotes the relative random fluctuation or systematic error. Here we make use of these correlated fluctuations to redistribute and compensate the energy gap fluctuations of the first-order dressed states (see Fig.1). With this we achieve that the energy

differences between dressed states are locked while the absolute energies may continue to fluctuate.

We apply the second-order driving to the first-order dressed Hamiltonian $H_I^{(1)} = \sqrt{2}\Omega_1(|u\rangle\langle u| - |d\rangle\langle d|)$ and obtain the following effective Hamiltonian in the second-order interaction picture as

$$H_I^{(2)} = \Omega_2 \left(\sqrt{10}|u\rangle\langle D| + \sqrt{10}|u\rangle\langle d| + |d\rangle\langle D| \right) + h.c. \quad (1)$$

The required continuous driving fields are equally separated in frequency by $\pm\sqrt{2}\Omega_1$ (see supplementary information for details). This makes it possible to generate these driving fields as sideband of the first-order driving field. Here, we choose different Rabi frequencies on purpose in order to break the degeneracy of the second-order dressed states (the ratio $\sqrt{10}$ is an example but it can take other values, see supplementary information for details), which can be written as $|d_1\rangle = \frac{\sqrt{2}}{3} \left(-\frac{5}{\sqrt{10}}|u\rangle + |D\rangle + |d\rangle \right)$, $|d_2\rangle = \frac{1}{6} (4|u\rangle + \sqrt{10}|D\rangle + \sqrt{10}|d\rangle)$, $|d_3\rangle = \frac{1}{\sqrt{2}} (-|D\rangle + |d\rangle)$, and the corresponding energies are $E_{d_1} = -4\Omega_2$, $E_{d_2} = 5\Omega_2$, $E_{d_3} = -\Omega_2$. The total energy fluctuations of the second-order dressed states can be calculated, by summing up the fluctuations from both the first and second order drivings, as $\delta E_{d_1}(t) = (-4\Omega_2 + \frac{\sqrt{2}}{3}\Omega_1)\delta(t)$, $\delta E_{d_2}(t) = (5\Omega_2 + \frac{\sqrt{2}}{6}\Omega_1)\delta(t)$, $\delta E_{d_3}(t) = (-\Omega_2 + \frac{\sqrt{2}}{2}\Omega_1)\delta(t)$. It can be seen that if we choose $\Omega_2 = \frac{\sqrt{2}}{54}\Omega_1$, the energy gap between $|d_1\rangle$ and $|d_2\rangle$ actually does not change over time, namely $\delta E_{d_1}(t) - \delta E_{d_2}(t) = 0$. Therefore, although the intensities of all the driving fields fluctuate and thus the individual energies of the second-order dressed states $|d_1\rangle$ and $|d_2\rangle$, the energy gap remains constant and the dephasing is effectively eliminated. The dressed states $|d_1\rangle$ and $|d_2\rangle$ therefore provide a qubit encoding that is inherently robust against both dephasing noise and intensity fluctuations. We remark that the fluctuation of the first-order driving may also cause transitions of the second-order dressed states, which is suppressed due to the energy penalty as long as the corresponding power spectrum of these fluctuations is negligible at the relevant transition frequency.

To demonstrate the robustness and efficiency of amplitude-lock CCD scheme, we consider NV center in diamond as an example. The electronic ground state of NV center has a spin one with three sublevels with magnetic quantum numbers $m_s = 0$ and $m_s = \pm 1$, and the zero field splitting is $\sim 2.87\text{GHz}$ [21]. One can apply an additional magnetic field to split the energy levels of $m_s = \pm 1$, so that the values of ω_+ and ω_- are different to allow selective microwave excitation of the $|0\rangle \leftrightarrow |+\rangle$ ($|0\rangle \leftrightarrow |-\rangle$) transitions. We numerically calculate the free decay of the transverse component of the electron spin $S_{01}(t) = |\rho_{01}(t)/\rho_{01}(0)|$ of a dressed qubit

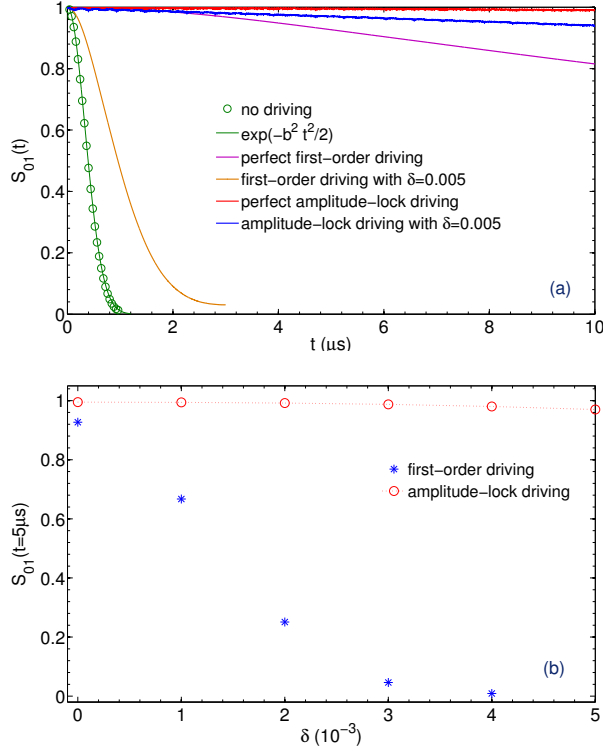


FIG. 2. (Color online) a: The free decay of the transverse component $S_{01}(t) = |\rho_{01}(t)/\rho_{01}(0)|$ for the qubit without driving, with first-order and second-order continuous dynamical decoupling. b: The signal S_{01} at $t = 5\mu s$ as a function of the relative intensity fluctuation δ . The magnetic noise is modeled as an Ornstein-Uhlenbeck process with the system-bath coupling strength $b = 3\mu s^{-1}$ and the bath correlation time $\tau_c = 25\mu s$. The amplitudes of driving fields are $\Omega_1 = 100\text{MHz}$ and $\Omega_2 = \frac{\sqrt{2}}{54}\Omega_1$. The parameters for the relative intensity fluctuation of driving fields are $\delta = 5 \times 10^{-3}(10^{-3})$ and $\tau_\Omega = 1\mu s$.

initially preparing a coherent superposition of $|d_1\rangle$ and $|d_2\rangle$. We compare the result with the electron-spin qubit (encoded with $|0\rangle$ and $|+\rangle$), as well as the first-order dressed qubit (encoded with $|u\rangle$ and $|d\rangle$). It was demonstrated that the dephasing process can be attributed to a random magnetic field $B(t)$ along the NV's quantization axis from the spin bath [26]. This random field $B(t)$ is well described by an Ornstein-Uhlenbeck process with the correlation function $C(t) = \langle B(0)B(t) \rangle = b^2 \exp(-|t|/\tau_c)$ [17], where b is the system-bath coupling strength and τ_c is the bath correlation time. The free decay of the transverse component of the electron spin has a Gaussian form $S(t) = \langle \exp(-i \int_0^t B(s)ds) \rangle = \exp(-b^2 t^2/2)$. The parameters for the spin bath are taken from the experimental estimations [17]: the coupling strength is $b = 3\mu s^{-1}$ and the correlation time is $\tau_c = 25\mu s$. The intensity of the driving field including its fluctuation is

$\Omega_i(t) = [1 + \delta(t)]\Omega_i$. As an example, we model the intensity fluctuation $\delta(t)$ also as an Ornstein-Uhlenbeck process. The results are obtained by averaging over 5000 realizations of $B(t)$ and $\delta(t)$. In Fig. 2 (a), it can be seen that the first-order dressing can indeed suppress the effect of magnetic noise. However, the unavoidable intensity fluctuations in the first-order driving fields would still cause dephasing and limit coherence times. With the second-order driving, the coherence time of the concatenated dressed qubit is significantly prolonged, exhibiting enhanced robustness against the intensity fluctuation of driving fields, see Fig.2 (b).

Dynamical decoupling not only increases coherence time of qubits, but also allow their efficient control using microwave fields. The coherent initialization, manipulation and readout of the encoded qubit with the concatenated dressed states $|d_1\rangle$ and $|d_2\rangle$ may be achieved in the following manner. The general coupling between the original states $|0\rangle, |\pm\rangle$ and a driving field is written as

$$H_c = g \exp(-i\omega_c t) (|-\rangle\langle 0| + |+\rangle\langle 0| + h.c.) \quad (2)$$

when the frequency of the driving field is $\omega_c = \omega_- - \sqrt{2}\Omega_1 + 9\Omega_2$, we get the required coupling that is on resonance with the transition between the dressed state $|d_1\rangle$ and $|d_2\rangle$ in the second-order interaction picture as $H_c^{(2)} = \left(\frac{5}{18\sqrt{2}}g\right) \exp[-i(E_{d_2} - E_{d_1})t] |d_2\rangle\langle d_1| + h.c.$, and the effective Rabi frequency is $g_e = \frac{5}{18\sqrt{2}}g$ (see supplementary information for details).

Sequential continuous dynamical decoupling — The amplitude-lock continuous driving scheme as discussed above is applicable for correlated intensity fluctuations. In the following, we introduce a complementary CCD scheme to counter independent fluctuations of driving fields. The principal idea is to provide a concatenated set of continuous driving fields with decreasing intensities such that each new driving field protects against the fluctuations of the driving field at the preceding

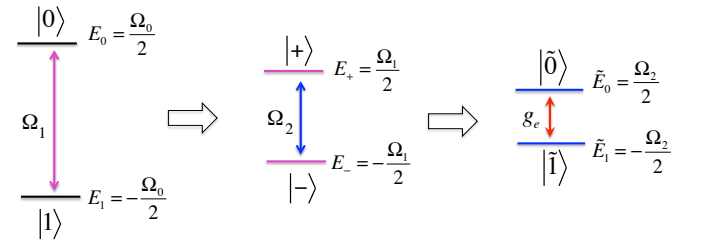


FIG. 3. Second-order sequential continuous dynamical decoupling: The first-order driving field Ω_1 creates the first-order dressed state $|+\rangle, |-\rangle$, and suppresses the dephasing effect of environment noise. The subsequent second-order driving Ω_2 overcomes the intensity fluctuation of the first-order driving field, and leads to the second-order dressed state that are subject to the reduced energy fluctuation.

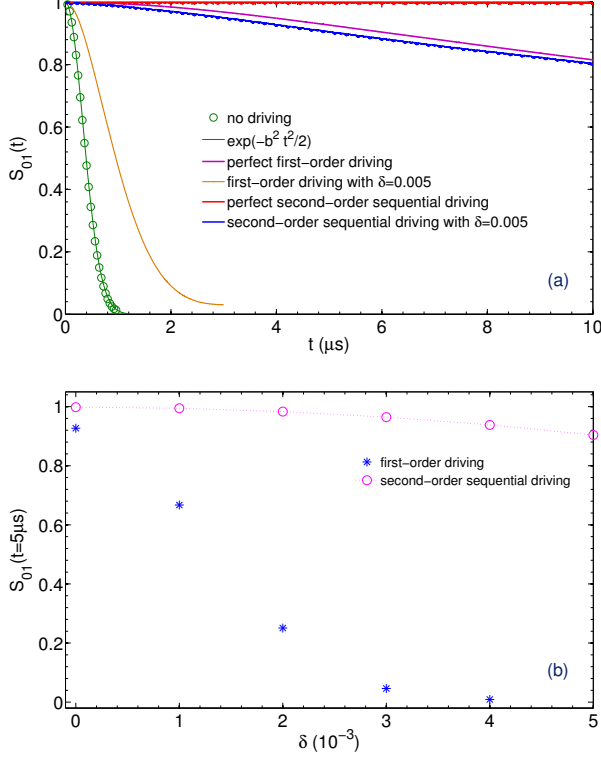


FIG. 4. (Color online) a: Comparison of free induction decay $S_{01}(t) = |\rho_{01}(t)/\rho_{01}(0)|$ in the cases of without driving, with first-order driving, and second-order sequential driving. b: The signal S_{01} at $t = 5\mu\text{s}$ as a function of the intensity fluctuation δ . The magnetic noise is modeled as an Ornstein-Uhlenbeck process with $b = 3\mu\text{s}^{-1}$ and $\tau_c = 25\mu\text{s}$. The driving fields are $\Omega_1/2\sqrt{2} = 100\text{MHz}$, and $\Omega_2/2\sqrt{2} = 10\text{MHz}$, which are chosen to make the first-order driving the same as in Fig. 2 for comparison. The parameters for the intensity fluctuation of the first- and second-order driving fields are $\delta = 5 \times 10^{-3}$ (10^{-3}), $\tau_\Omega = 1\mu\text{s}$.

level. We consider a simple two-level quantum system $H_0 = \frac{\Omega_0}{2}(|0\rangle\langle 0| - |1\rangle\langle 1|)$. The dephasing noise δ_0 leads to the loss of coherence of a qubit encoded in the states $|0\rangle, |1\rangle$. With the first-order driving

$$H_{d1} = \Omega_1 \cos(\Omega_0 t) X \quad (3)$$

where $X = |0\rangle\langle 1| + |1\rangle\langle 0|$, in the first-order interaction picture with rotating wave approximation, we get $H_I^{(1)} = \frac{\Omega_1}{2}(|+\rangle\langle +| - |-\rangle\langle -|)$, where $|\pm\rangle = \frac{1}{\sqrt{2}}(|0\rangle \pm |1\rangle)$ are the first-order dressed states. The fluctuation δ_1 in the driving Ω_1 can be suppressed by applying a second-order driving field as follow

$$H_{d2} = \Omega_2 \cos(\Omega_1 t) Z. \quad (4)$$

We remark that similar results are obtained if the second-order driving consists of Y component. If the intensity fluctuation of the driving field $\delta_1 \ll \delta_0$, it is sufficient

for us to apply a second-order driving with $\Omega_2 \ll \Omega_1$ to eliminate the impact of the intensity fluctuation δ_1 . With these two driving fields as in Eq.(5-6), we get the effective Hamiltonian in the second-order interaction picture as $H_I^{(2)} = \Omega_2(|\tilde{0}\rangle\langle \tilde{0}| - |\tilde{1}\rangle\langle \tilde{1}|)$. The energy gap fluctuation for the second-order dressed states is thus reduced to δ_2 which is much smaller than δ_1 . In general, we can apply n -order continuous driving fields (on the condition that two subsequent drivings anti-commute with each other, that is they describe rotations about orthogonal axes.) and reduce the effective intensity fluctuation in a sequential way. As the dephasing of the n -th order dressed qubit originates mainly from the fluctuations of the n -th order driving field, the coherence time may be extended significantly, see Fig.4. The scheme is also robust against (small) unwanted components in the driving fields, for example Y, Z components and X, Y components in the first- and second-order drivings respectively (see supplementary information for details). It should be noted that this CCD scheme is closely related to composite pulse techniques that have been developed in NMR [30]

The initialization, coherent manipulation and readout for the second-order dressed qubit can be achieved with a continuous driving field at the frequency $\omega_c = \Omega_0 + \Omega_2$ (see supplementary information for details). Such a qubit encoded with the sequential dressed states has an ultra-long coherence time, and thereby can be exploited to construct a single-spin magnetometer to probe a weak magnetic field in the \hat{z} direction oscillating at a frequency $\omega = \Omega_1$. In the second-order interaction picture, it is equivalent to a static magnetic acting on the dressed qubit. One can tune the functioning frequency by changing the Rabi frequency Ω_1 of the driving field. The magnetic field sensitivity is $\eta = \hbar / (g\mu_B \sqrt{T_2 T})$ where T_2 is the coherence time, T is the measurement time. With the prolonged coherence time T_2 , the magnetic field sensitivity is expected to be significantly enhanced [31]. It can also be exploited to measure noise spectra [32] with a high precision.

The idea of sequential driving can also be used to implement fault-tolerant single qubit rotation $R(\theta, \phi) = \exp(-i\theta\sigma_\phi)$, where $\sigma_\phi = \cos(\phi)X + \sin(\phi)Y$ and X, Y are Pauli operators. We start from the Hamiltonian for rotation $H_0 = \frac{\Omega_0}{2}(1 + \epsilon_0)\sigma_\phi$, which generates a rotation $R(\theta + \theta\epsilon_0, \phi)$ with the angle error $\theta\epsilon_0$ during time $[0, 2\theta/\Omega_0]$. Applying two driving fields as $H_d^{(1)} = \frac{\Omega_1}{2}(1 + \epsilon_1)\cos(\Omega_0 t)Z$, $H_d^{(2)} = \frac{\Omega_2}{2}(1 + \epsilon_2)\cos(\Omega_1 t)\sigma_\phi$ in time $[2\theta/\Omega_0, 4\theta/\Omega_0]$, and choosing $\Omega_1 = (\frac{\pi}{\theta})\Omega_0$, then the total time evolution during $[0, 4\theta/\Omega_0]$ gives us $R_\phi(-\theta\epsilon_0)Z$, which can be used to compensate the angle error [30].

Summary.— We have introduced the method of concatenated continuous dynamical decoupling, and propose two complementary schemes of amplitude-lock concatenated driving fields and sequential concatenated driving

fields. We demonstrate the superior performance of concatenated continuous dynamical decoupling compared to single driving fields in extending coherence times of a dressed qubit, as a qubit encoded in the concatenated dressed states is robust against both dephasing noise and intensity fluctuation of driving fields. Our schemes can be applied to a wide variety of quantum systems where they may find applications in the construction of nanoscale magnetometry e.g. with NV center in diamond, and in the construction of fault-tolerant quantum gates that are protected against noise and control errors.

Acknowledgements The work was supported by the Alexander von Humboldt Foundation, the EU Integrating Project Q-ESSENCE, the EU STREP PICC and DIAMANT, the BMBF Verbundprojekt QuOREP, DFG (FOR 1482 and 1493) and DARPA. J.-M.C was supported also by a Marie-Curie Intra-European Fellowship within the 7th European Community Framework Programme. We acknowledge the bwGRiD for computational resources.

-
- [1] J. R. Maze, *et. al.*, Nature **455**, 644 (2008).
 - [2] G. Balasubramanian, *et. al.*, Nature **455**, 648 (2008).
 - [3] G. de Lange, D. Riste, V. V. Dobrovitski, and R. Hanson, Phys. Rev. Lett. **106**, 080802 (2011).
 - [4] J. A. Jones et al., Science **324**, 1166 (2009).
 - [5] W. H. Zurek Nature Physics **5**, 181 (2009).
 - [6] E. L. Hahn, Phys. Rev. **80**, 580594 (1950).
 - [7] L. Viola and S. Lloyd, Phys. Rev. A **58**, 2733 (1998).
 - [8] P. Facchi, D. A. Lidar, and S. Pascazio, Phys. Rev. A **69**, 032314 (2004)
 - [9] K. Khodjasteh and D. A. Lidar, Phys. Rev. Lett. **95**, 180501 (2005) .
 - [10] G. S. Uhrig, Phys. Rev. Lett. **98**, 100504 (2007).
 - [11] P. Rabl, P. Cappellaro, M. V. Gurudev Dutt, L. Jiang, J. R. Maze, and M. D. Lukin, Phys. Rev. B **79**, 041302 (2009).
 - [12] A. Bermudez, F. Jelezko, M. B. Plenio, A. Retzker, Phys. Rev. Lett. **107**, 150503 (2011).
 - [13] A. Bermudez, P. O. Schmidt, M. B. Plenio, A. Retzker, arXiv:1110.1870.
 - [14] N. Timoney, V. Elman, S. Glaser, C. Weiss, M. Johanning, W. Neuhauser, and Chr. Wunderlich, Phys. Rev. A **77**, 052334 (2008).
 - [15] M. J. Biercuk, H. Uys, A. P. VanDevender, N. Shiga, W. M. Itano and J. J. Bollinger, Nature **458**, 996-1000 (2009).
 - [16] J. Du, X. Rong, N. Zhao, Y. Wang, J. Yang and R. B. Liu, Nature **461**, 1265-1268 (2009).
 - [17] G. de Lange, Z. H. Wang, D. Riste, V. V. Dobrovitski, R. Hanson, Science **330**, 60 (2010).
 - [18] C. A. Ryan, J. S. Hodges, and D. G. Cory, Phys. Rev. Lett. **105**, 200402 (2010).
 - [19] A. M. Souza, G. A. Alvarez, and D. Suter, Phys. Rev. Lett. **106**, 240501 (2011).
 - [20] N. Timoney, I. Baumgart, M. Johanning, A. F. Varon, M. B. Plenio, A. Retzker, Ch. Wunderlich, Nature **476**, 185-188 (2011).
 - [21] J. Wrachtrup and F. Jelezko, J. Phys.: Condens. Matter **18**, S807-824 (2006).
 - [22] F. Jelezko, T. Gaebel, I. Popa, M. Domhan, A. Gruber, and J. Wrachtrup, Phys. Rev. Lett. **93**, 130501 (2004).
 - [23] L. Jiang, J. S. Hodges, J. Maze, P. Maurer, J. M. Taylor, A. S. Zibrov, P. R. Hemmer, and M. D. Lukin, Science **326**, 267 (2009).
 - [24] P. Neumann et al., Nature Physics **6**, 249 (2010).
 - [25] L. Childress, M. V. Gurudev Dutt, J. M. Taylor, A. S. Zibrov, F. Jelezko, J. Wrachtrup, P. R. Hemmer and M. D. Lukin, Science **314**, 281 (2006).
 - [26] R. Hanson, V. V. Dobrovitski, A. E. Feiguin, O. Gywat, Science **320**, 352 (2008).
 - [27] G. Balasubramanian, *et. al.*, Nature Materials **8**, 383 - 387 (2009).
 - [28] G. D. Fuchs, G. Burkard, P. V. Klimov and D. D. Awschalom, Nature Physics **7**, 789-793 (2011).
 - [29] H. Fedder, F. Dolde, F. Rempp, T. Wolf, P. Hemmer, F. Jelezko, J. Wrachtrup, Applied Physics B: Lasers and Optics **102**, 497-502 (2010).
 - [30] Kenneth R. Brown, Aram W. Harrow, and Isaac L. Chuang, Phys. Rev. A **70**, 052318 (2004).
 - [31] J. M. Taylor, P. Cappellaro, L. Childress, L. Jiang, D. Budker, P. R. Hemmer, A. Yacoby, R. Walsworth and M. D. Lukin, Nature Physics **4**, 810 (2008).
 - [32] T. Yuge, S. Sasaki, and Y. Hirayama, Phys. Rev. Lett. **107**, 170504 (2011).

SUPPLEMENTARY MATERIAL

Continuous driving fields for amplitude-lock CCD scheme.— The bare Hamiltonian of a three-level system is

$$H_0 = (\omega_- |-\rangle \langle -| + \omega_+ |+\rangle \langle +|) \quad (5)$$

By applying the first-order driving field $H_{d_1} = \Omega_1 (|-\rangle \langle 0| e^{-i\omega_- t} + |+\rangle \langle 0| e^{-i\omega_+ t}) + h.c.$, we get the following Hamiltonian in the first-order interaction picture with respect to H_0 as

$$H_I^{(1)} = \sqrt{2}\Omega_1 (|u\rangle \langle u| - |d\rangle \langle d|) \quad (6)$$

where the first-order dressed states are

$$|u\rangle = (|+\rangle + |-\rangle + \sqrt{2}|0\rangle)/2, \quad |d\rangle = (|+\rangle + |-\rangle - \sqrt{2}|0\rangle)/2, \quad |D\rangle = (|+\rangle - |-\rangle)/\sqrt{2}. \quad (7)$$

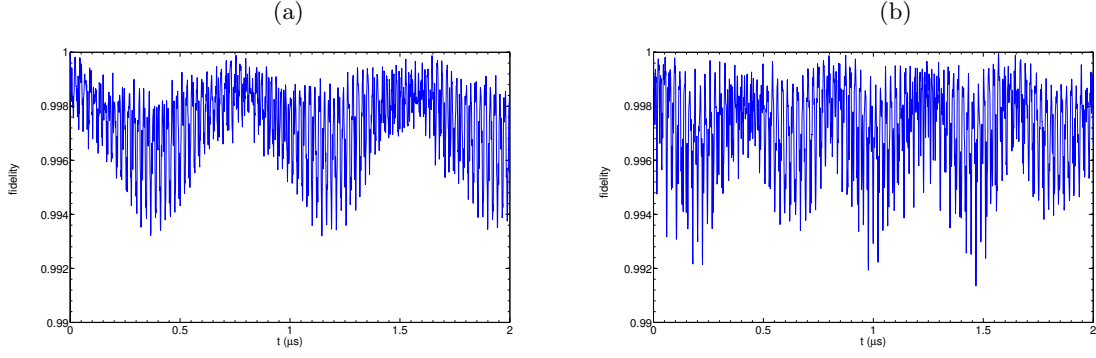


FIG. 5. Verification of the rotating wave approximation (RWA). The state fidelity $f = \langle \psi(0) | \rho(t) | \psi(0) \rangle$ as a function of time t starting from the second-order dressed state $|\psi(0)\rangle = |d_1\rangle$ (a) and $|d_2\rangle$ (b).

The continuous driving fields required for the second-order dressing is given by

$$H_{d_2}^{(ud)} = -\sqrt{20}\Omega_2 \left[|+\rangle \langle 0| e^{-i(\omega_+ + 2\sqrt{2}\Omega_1)t} + |-\rangle \langle 0| e^{-i(\omega_- + 2\sqrt{2}\Omega_1)t} \right] + h.c.. \quad (8)$$

In the first-order interaction picture, it drives Rabi transition between the dressed states $|u\rangle$ and $|d\rangle$, i.e. $H_I^{(ud)} = \sqrt{10}\Omega_2 \left(e^{-i2\sqrt{2}\Omega_1 t} |u\rangle \langle d| + e^{i2\sqrt{2}\Omega_1 t} |d\rangle \langle u| \right)$. This leads to the term $\sqrt{10}\Omega_2 (|u\rangle \langle d| + |d\rangle \langle u|)$ of the effective Hamiltonian (see Eq.(1) in the main text) in the second-order interaction picture with respect to $H_I^{(1)}$. In a similar way, the transition between the first-order dressed states $|u\rangle$ and $|D\rangle$ is achieved by applying another driving field as

$$H_{d_2}^{(uD)} = -\sqrt{10}\Omega_2 \left[|-\rangle \langle 0| e^{-i(\omega_- - \sqrt{2}\Omega_1)t} - |+\rangle \langle 0| e^{-i(\omega_+ - \sqrt{2}\Omega_1)t} \right] + h.c. \quad (9)$$

and the driving between $|d\rangle$ and $|D\rangle$ by

$$H_{d_2}^{(dD)} = \Omega_2 \left[|-\rangle \langle 0| e^{-i(\omega_- + \sqrt{2}\Omega_1)t} - |+\rangle \langle 0| e^{-i(\omega_+ + \sqrt{2}\Omega_1)t} \right] + h.c. \quad (10)$$

which give us the terms $\sqrt{10}\Omega_2 (|u\rangle \langle D| + |D\rangle \langle u|)$ and $\Omega_2 (|d\rangle \langle D| + |D\rangle \langle d|)$ of the effective Hamiltonian in the second-order interaction picture. The frequencies of these driving fields are equally separated by $\sqrt{2}\Omega_1$. This make it possible to generate these driving fields as sideband from the first-order driving field. One may note that the Rabi frequencies here are chosen to be different. In fact, if they are all the same, we obtain two degenerate second-order dressed states, which make it inconvenient to use them to encode a qubit. We set the ratio between Rabi frequencies as $\sqrt{10}$, but it can also take other values. This ratio determines the amplitude of Ω_2 (compared to Ω_1) based on Eq.(2) in the main text. The only constraint for the ratio is that it should satisfy the rotating wave approximation (RWA) in the second-order drivings, otherwise they may cause unwanted transitions. For the specific value of $\sqrt{10}$, we have verified that the RWA condition is well satisfied, see Fig.5.

Coherent manipulation of the dressed qubit in amplitude-lock CCD scheme.— If we want to encode a qubit into the second-order dressed state, it is necessary to be able to perform initialization, coherent manipulation, and readout on the encoded qubit. We propose to use a driving field with the frequency $\omega_c = \omega_- - \sqrt{2}\Omega_1 + 9\Omega_2$ as follows

$$H_c = g \exp(-i\omega_c t) (|-\rangle \langle 0| + |+\rangle \langle 0| + h.c.). \quad (11)$$

In the first-order interaction picture with respect to H_0 , the field-qubit interaction can be written as

$$H_c^{(1)} = g \left[e^{i(\sqrt{2}\Omega_1 - 9\Omega_2)t} \left(\frac{1}{2\sqrt{2}} (|u\rangle \langle u| - |u\rangle \langle d| + |d\rangle \langle u| - |d\rangle \langle d|) - \frac{1}{2} (|D\rangle \langle u| - |D\rangle \langle d|) \right) + h.c. \right]. \quad (12)$$

In the second order interaction picture with respect to $H_I^{(1)}$, it is transformed as

$$H_c^{(2)} = \left(\frac{5}{18\sqrt{2}} g \right) (e^{-i9\Omega_2 t} |d_2\rangle \langle d_1| + e^{i9\Omega_2 t} |d_1\rangle \langle d_2|) \quad (13)$$

where we have used the rotating wave approximation (RWA). One also note that the energy gap for the dressed qubit is $E_{d_2} - E_{d_1} = 9\Omega_2$. Therefore, the effective coupling in Eq.(14) will induce Rabi oscillation of the dressed qubit.

Robustness of sequential CCD scheme.— If there is a small (but known) Y component in the first-order driving, we can redefine the X operator and will not affect the efficiency of the scheme. We consider the situation when there is a small Z component in the first-order driving which now is written as

$$H_{d_1} = \Omega_1 \cos(\Omega_0 t) X + \Omega_1^z \cos(\Omega_0 t) Z. \quad (14)$$

In the first-order interaction picture with respect to the original Hamiltonian $H_0 = \frac{\Omega_0}{2} (|0\rangle\langle 0| - |1\rangle\langle 1|)$, the effective Hamiltonian is

$$H_I^{(1)} = \Omega_1 X + \Omega_1^z \cos(\Omega_0 t) Z. \quad (15)$$

If the condition $\Omega_1^z \ll \Omega_0 \pm \Omega_1$ is satisfied, the fast oscillatory Z component will be averaged out and can be neglected. We further assume that there are X and Y component in the second-order driving as follows

$$H_{d_2} = \Omega_2 \cos(\Omega_1 t) Z + \Omega_2^x \cos(\Omega_1 t) X + \Omega_2^y \cos(\Omega_1 t) Y. \quad (16)$$

In the second-order interaction picture, the effective Hamiltonian becomes

$$H_I^{(2)} = \Omega_2 Z + \cos(\Omega_1 t) \{ [\Omega_2^x \cos(\Omega_0 t) + \Omega_2^y \sin(\Omega_0 t)] X + [\Omega_2^y \cos(\Omega_0 t) - \Omega_2^x \sin(\Omega_0 t)] [\cos(\Omega_1 t) Y - \sin(\Omega_1 t) Z] \}. \quad (17)$$

It can be seen that the effect of X and Y component will also be average out if $\Omega_2^x, \Omega_2^y \ll \Omega_0$. Therefore, the sequential continuous dynamical decoupling scheme is robust against (small) unwanted components in the driving fields, for example Y, Z components and X, Y components in the first- and second-order drivings respectively.

Coherent manipulation of the dressed qubit in sequential CCD scheme.— The dressed qubit can be manipulated by a driving field with the frequency $\omega_c = \Omega_0 + \Omega_2$ as

$$H_c = g \cos(\omega_c t) X \quad (18)$$

where X is the Pauli operator. In the first-order interaction picture with respect to the original Hamiltonian $H_0 = \frac{\Omega_0}{2} (|0\rangle\langle 0| - |1\rangle\langle 1|)$, under the RWA condition ($g \ll 2\Omega_0 + \Omega_2$), the coupling can be written as

$$H_c^{(1)} = \frac{g}{2} [\exp(-i\Omega_2 t) |0\rangle\langle 1| + \exp(-i\Omega_2 t) |1\rangle\langle 0|] \quad (19)$$

In the second order interaction picture with respect to $H_I^{(1)} = \frac{\Omega_1}{2} (|+\rangle\langle +| - |-\rangle\langle -|)$, under the RWA condition ($\frac{g}{2} \ll \Omega_1 \pm \Omega_2$), it is transformed to

$$H_c^{(2)} = \frac{g}{2} \cos(\Omega_2 t) X \quad (20)$$

which induces Rabi oscillation between the second-order dressed states.